# Total oxidation of propane over Cu-Mn mixed oxide catalysts prepared by co-precipitation method

**Moon Hyeon Kim\*, Kyung Ho Cho\*\*, Chae-Ho Shin\*\*, Seong-Eun Kang\*\*\*, and Sung-Won Ham\*\*\*,†**

\*Department of Environmental Engineering, Daegu University, Gyeongsan 712-714, Korea
\*\*Department of Chemical Engineering, Chungbuk National University, Cheongju, Chungbuk 361-763, Korea
\*\*\*Department of Chemical Engineering, Kyungil University, Gyeongsan 712-701, Korea

**Abstract**−The catalytic activity of Cu-Mn mixed oxides with varying Cu/Mn ratios prepared by co-precipitation method was examined for the total oxidation of propane. The nature and phase of the metal oxide species formed were characterized by various methods such as X-ray diffraction (XRD), X-ray photoelectron spectroscopy (XPS), $H_2$ temperature-programmed reduction (TPR) as well as BET surface area measurement. The co-precipitation method provides highly interdispersed copper and manganese metallic elements forming Cu-Mn mixed oxide of spinel structure ($Cu_{1.5}Mn_{1.5}O_4$). Besides the spinel-type Cu-Mn mixed oxide, CuO or $Mn_2O_3$ phases could be formed depending on the Cu/Mn molar ratio of their precursors. The catalytic activity of Cu-Mn mixed oxide catalyst for propane oxidation was much higher than those of single metal oxides of CuO and $Mn_2O_3$. The higher catalytic activity likely originates from a synergic effect of spinel-type Cu-Mn mixed oxide and CuO. The easier reducibility and BET surface area seems to be partially responsible for the high activity of Cu-Mn mixed oxide for total oxidation of propane.

Key words: Propane Oxidation, Cu-Mn Mixed Oxide, Co-precipitation, $H_2$ Temperature-programmed Reduction

## INTRODUCTION

Total catalytic oxidation technology has been widely used in several processes for air pollution abatement, especially for controlling hydrocarbon emissions, VOCs (volatile organic compounds) and carbon monoxide [1,2]. Major emission sources of the compounds are vehicles and various industrial sites such as plants manufacturing organic chemicals, polymers or synthetic fibers and smaller units such as painting and coating operations. Recently, environmental legislation in the world is posing stringent standards on VOC emissions, the satisfaction of which requires improvement of the efficiency of VOCs removal technologies [3].

Noble metals such as palladium and platinum are the most commonly used as catalysts for total oxidation of hydrocarbons, VOCs and carbon monoxide [1,3-7]. Because of the high cost and limited availability of noble metals [8], however, many efforts have been made for the development of catalysts based on transition-metal mixed oxides [9]. In particular, catalysts based on copper-manganese mixed oxide are of considerable industrial interest due to their high activity as oxidation catalysts. The copper-manganese mixed oxide catalysts can catalyze oxidation reactions such as carbon monoxide [10-16], organic compounds including hydrocarbons [4,17], halide and nitrogen-containing compounds [18,19] and the water-gas shift reaction [20,21].

The success of the copper-manganese mixed oxide catalyst has prompted a great deal of fundamental work to clarify the role played by each component and the nature of the active sites. This has been extensively documented in several reviews [22-24]. However, many controversial issues such as the nature of active sites and the role played by each component in the mixed oxide catalyst remain to be resolved. The activity of copper-manganese oxide is known to significantly depend upon the structure of the catalyst precursor, and this is in turn controlled by the preparation route. The effect of the preparation conditions on the catalytic activity of copper-manganese oxide catalyst has been shown to be of great importance and effective catalysts are typically prepared using co-precipitation from the mixed nitrates [13]. Experimental variables during the precipitation such as pH, temperature, Cu/Mn ratio and the precipitate ageing as well as the treatment of the initial precursor by calcinations have all been shown to be crucial [25]. Optimum preparation conditions have been identified in terms of producing the highest activity for the reaction.

Among the various important aspects of preparation conditions, we focused on the Cu/Mn ratios of copper manganese mixed oxide. To understand the nature of Cu-Mn mixed oxide catalyst for hydrocarbon oxidation, we used propane as a model gas since it is one of the stable lower alkanes requiring high temperatures to be completely oxidized [26]. The phase compositions and the nature of copper-manganese mixed oxide prepared by co-precipitation method were investigated with the help of the XRD, XPS, $H_2$-TPR and BET measurements. The catalytic activity of Cu-Mn mixed oxide for the total oxidation of propane was examined and discussed in view of the physicochemical properties such as phase and chemical compositions, reducibility and BET surface area of the catalyst.

## EXPERIMENTAL

### 1. Catalyst Preparation

Copper manganese mixed oxide catalysts with Cu/Mn molar ratios

---

†To whom correspondence should be addressed.
E-mail: swham@kiu.ac.kr

equal to 15/85, 50/50, 85/15 were prepared by a co-precipitation method. Aqueous solutions of 0.25 mol/$l$ Cu(NO$_3$)$_2$·2.5H$_2$O (Sigma-Aldrich) and 0.25 mol/$l$ Mn(NO$_3$)$_2$·6H$_2$O (Sigma-Aldrich) were pre-mixed according to the desired Cu/Mn molar ratio. Aqueous solution of 0.25 mol/$l$ Na$_2$CO$_3$ used as a precipitating agent was added to the mixed nitrate solution, which was continuously agitated and maintained within the temperature range of 25-30 °C. The precipitate was then filtered, washed several times with distilled water until no further Na$^+$ was observed in the washing. The precipitate was dried at 120 °C over night, followed by calcination at 500 °C for 12 h. Single metal oxides of copper and manganese were also prepared by the aforementioned procedures. The resulting catalysts were denoted as CuA-MnB, where A, B were the relative molar ratio in percentage of copper and manganese in the catalyst, respectively.

## 2. Catalyst Characterization

A Micromeritics ASAP 2010 analyzer was used to measure the N$_2$ adsorption isotherms of the samples at liquid N$_2$ temperature (–196 °C). The BET surface area was calculated from the linear portion of the BET plot. Prior to the measurement of the surface area, the sample was degassed in vacuum at 250 °C for at least 4 h.

The powder diffraction patterns for the copper manganese mixed oxides were obtained with an automated PANanalytical X'Pert PRO diffractometer. Scans were taken with a 2$\theta$ step size of 0.01°, using a Cu K$\alpha$ radiation generated at 40 kV and 30 mA of X-ray gun. The phases of components in catalysts were identified by matching diffraction patterns to the JCPDS powder diffraction file.

X-ray photoelectron spectroscopy (XPS) was used to determine the chemical state of the elements on catalyst by a VG ESCALAB 250. The Al K$\alpha$ X-ray (1486.6 eV) radiation was operated at 15 kV and 15 mA as the excitation source. Charging of samples was corrected by setting the binding energy of C 1s peak at 284.6 eV.

H$_2$ temperature-programmed reduction (H$_2$-TPR) spectra were obtained with a Micromeritics AutoChem II 2920 with a TCD (thermal conductivity detector). A 20 mg sample was loaded in a quartz U-type tubular reactor. The reducing gas was a mixture of 5% H$_2$/Ar at a total flow rate of 50 ml/min. The temperature was increased at a rate of 10 °C/min from room temperature to 700 °C during the TPR measurement.

## 3. Reactor System for Catalyst Activity Measurement

Catalytic activity for total oxidation of propane to CO$_2$ was examined in a fixed bed reactor, typically containing 0.3 g of powder catalyst placed in a quartz tube reactor. A gas mixture of 200 ml/min containing 1% C$_3$H$_8$, 7% O$_2$ in He balance was fed to the reactor system through mass flow controller (Brooks Model 5850E). The reactants and products were analyzed by on-line gas chromatography of an Agilent 6890 GC system equipped with TCD and a craboxen-1000 column.

## RESULTS AND DISCUSSION

### 1. XRD Measurement

To identify the phase compositions of copper manganese mixed oxides prepared by co-precipitation method, XRD measurements were performed for the catalysts with different Cu/Mn molar ratios as shown in Fig. 1. Single metal oxides of copper and manganese prepared following the same synthesis method employed to the mixed oxides were included as reference samples in Fig. 1. The sample
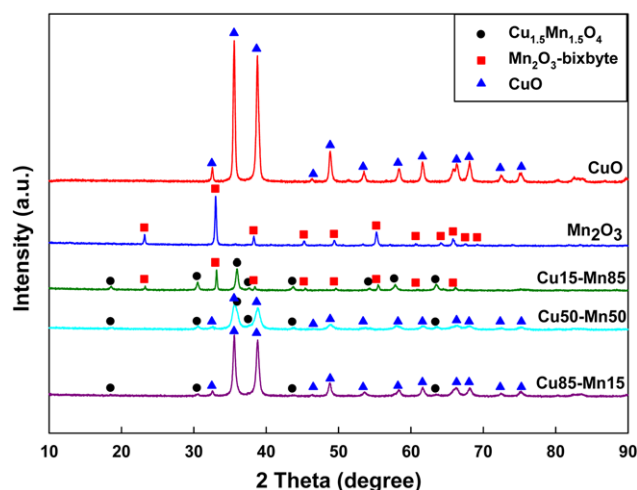
Fig. 1. XRD patterns of single metal oxides and Cu-Mn mixed oxide catalysts prepared by co-precipitation method.

Table 1. Observed crystalline phases and crystalline size of CuO in Cu-Mn mixed oxide catalysts after calcination in air at 500 °C for 12 h

| Catalysts | Crystalline phases | Crystalline size of CuO (nm) |
| --- | --- | --- |
| Cu15-Mn85 | Mn$_2$O$_3$, Cu$_{1.5}$Mn$_{1.5}$O$_4$ | ND |
| Cu50-Mn50 | CuO, Cu$_{1.5}$Mn$_{1.5}$O$_4$ | 10.4 |
| Cu85-Mn15 | CuO, Cu$_{1.5}$Mn$_{1.5}$O$_4$ | 21.8 |

ND: not detected

obtained from the solution containing only copper nitrate was confirmed to be CuO (JCPDS 89-2529). Crystalline $\alpha$-Mn$_2$O$_3$ (JCPDS 89-4836) can be obtained in the copper-free sample prepared by the solution containing only manganese nitrate. The results of XRD show the diffraction lines of Mn$_2$O$_3$, CuO and Cu$_{1.5}$Mn$_{1.5}$O$_4$ in the mixed oxide samples. As summarized in Table 1, the dominant phases of metal species were significantly dependent on the molar ratio of Cu/Mn. The catalyst obtained by co-precipitation with a molar ratio of Cu/Mn=1 (Cu50-Mn50 sample) was constituted of Cu$_{1.5}$Mn$_{1.5}$O$_4$ (JCPDS 70-0260) phase and CuO. The diffraction lines indicated the spinel type Cu$_{1.5}$Mn$_{1.5}$O$_4$ mixed oxide was much less crystalline than CuO phase. The CuO phase became more crystalline, producing narrow and highly intense diffraction lines with the increase of the molar ratio of Cu/Mn. The crystalline sizes of CuO calculated by the Scherrer equation in Cu50-Mn50 and Cu85-Mn15 samples were 10.4 and 21.8 nm, respectively, which were smaller than that of CuO sample (23.1 nm). In contrast, Cu15-Mn85 sample prepared by co-precipitation with much lower Cu/Mn molar ratio than 1 showed the Cu$_{1.5}$Mn$_{1.5}$O$_4$ mixed oxide and Mn$_2$O$_3$ phase. CuO phase was not detected by XRD. This result indicates that the co-precipitation method used for the synthesis of catalysts provides a high interdispersion of copper and manganese metallic elements forming Cu-Mn mixed oxide of spinel type (Cu$_{1.5}$Mn$_{1.5}$O$_4$). Besides the spinel-type Cu-Mn mixed oxide, CuO or Mn$_2$O$_3$ phases could be formed depending on the Cu/Mn molar ratio of their precursors.

### 2. XPS Measurement

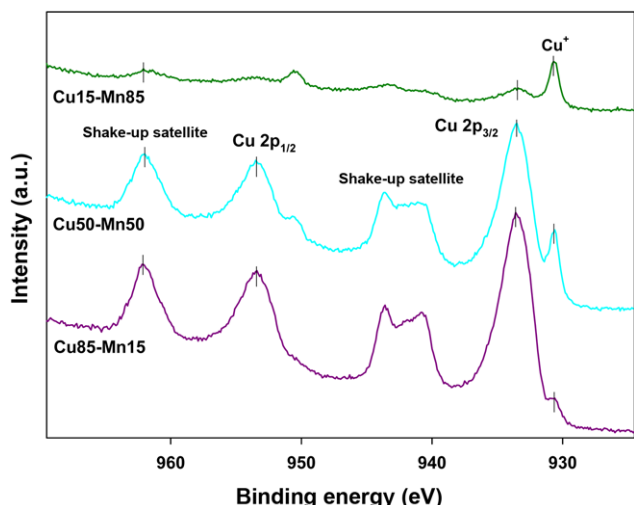XPS spectra can give good information on the chemical state of

**Fig. 2. Cu 2p XPS spectra of Cu-Mn mixed oxide catalysts.**

components in catalyst. Fig. 2 shows Cu 2p XPS spectra of the Cu-Mn mixed oxide catalysts with different Cu/Mn molar ratio. The observation of the Cu $2p_{3/2}$ at 933.5 eV and Cu $2p_{1/2}$ at 953.5 eV of binding energy obviously indicates the existence of $Cu^{2+}$. The shake-up satellites corresponding to Cu 2p also confirm the presence of $Cu^{2+}$. They do not appear in $Cu^+$ or $Cu^0$ species, since shake-up transitions do not occur in filled 3d shells and metallic states [18]. The peak intensity for $Cu^{2+}$ was very small on the catalyst of Cu15-Mn-85. As already identified by XRD measurement, CuO phase was not observed on the Mn-rich Cu15-Mn-85 catalyst. Therefore, the strong $Cu^{2+}$ peak seems to be mainly originated from the CuO phase.

For all the catalysts, Cu 2p peak also appears at the binding energy of 930.6 eV, which is the $Cu^+$ occupying the tetrahedral sites of the spinel structure. The existence of $Cu^+$ on the Cu-Mn mixed oxide indicates the formation of Cu-Mn spinel structure, regardless of the Cu/Mn molar ratios during the preparation of mixed oxide. This result is in good agreement with the XRD showing the presence of spinel structure of Cu-Mn oxide.

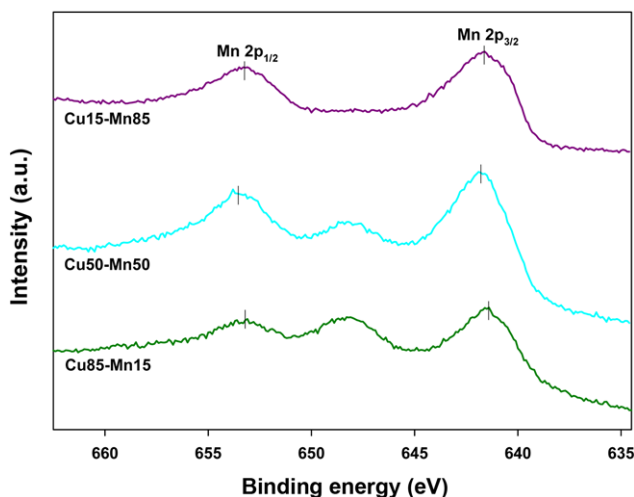Fig. 3 shows the Mm 2p XPS spectra of Cu-Mn mixed oxide

catalysts which are the same as the catalysts examined in Fig. 2. For all the catalysts, the binding energies for Mn $2p_{3/2}$ appear at 641.6-641.8 eV and those for Mn $2p_{1/2}$ appear at 653.2-653.7 eV. Since the difference in binding energy of $Mn^{2+}$, $Mn^{3+}$ and $Mn^{4+}$ is small, it is very difficult to precisely determine the oxidation states of Mn. From the XRD measurements, it is identified that $Mn_2O_3$ phase exists only in the Cu15-Mn85 catalyst, while spinel structure of Cu-Mn mixed oxide exists in all the catalysts. The spinel contains mainly $Mn^{3+}$, but also $Mn^{4+}$ according to the equilibrium between $Cu^{2+}$, $Mn^{3+}$ and $Cu^+$, $Mn^{4+}$ ($Cu^{2+}+Mn^{3+}\leftrightarrow Cu^++Mn^{4+}$). Therefore, it is expected that both $Mn^{3+}$ and $Mn^{4+}$ can exist in all catalysts, although oxidation state of Mn is hard to distinguish by XPS measurement in this study.

### 3. H$_2$-TPR Measurement

The reducibility of the catalysts was determined by H$_2$-TPR measurement as shown in Fig. 4. The reduction of CuO sample prepared by precipitation method in this study occurs in one step that probably corresponds to the reduction of CuO to $Cu^0$ at the temperature maximum of 226 °C. The reduction of $Mn_2O_3$ sample exhibits two well-defined peaks with the maxima at 273 and 365 °C. The first peak is probably attributed to the reduction of $Mn_2O_3$ to $Mn_3O_4$ and the higher temperature peak can be related to the further reduction of $Mn_3O_4$ to MnO. For thermodynamic reasons, further reduction of MnO does not occur under our experimental condition [27].

The Cu-Mn mixed oxides show different reduction behaviors with respect to Cu/Mn molar ratio. The Mn-rich catalyst, Cu15-Mn85, reveals two step reductions which are similar to the single oxide of $Mn_2O_3$. $Mn_2O_3$ was observed as main component in Cu15-Mn85 catalyst. Therefore, the reduction peaks of Cu15-Mn85 catalyst are considered as the reduction of $Mn_2O_3$ in two steps same as those of single metal oxide of $Mn_2O_3$. However, two peak maxima appear at much lower temperatures than the single oxide of $Mn_2O_3$, indicating the improved reducibility. The reduction of Cu50-Mn50 and Cu-rich Cu85-Mn15 occurs in one step that seems to be attributed to the reduction of CuO to metallic copper. The main component of these two catalysts was confirmed as CuO by XRD measure-
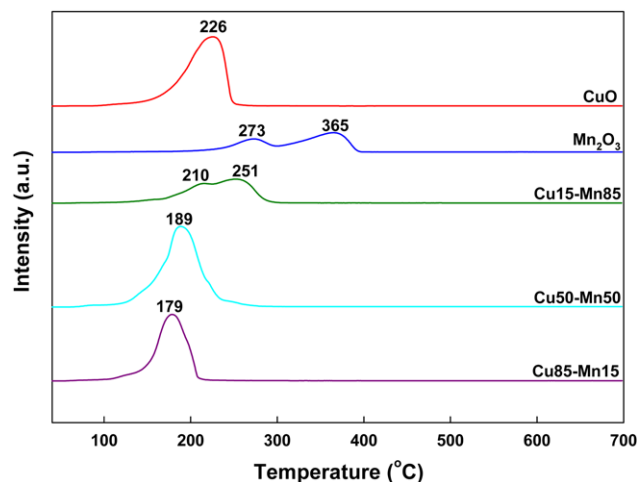


**Fig. 3. Mn 2p XPS spectra of Cu-Mn mixed oxide catalysts.**



**Fig. 4. H$_2$-TPR profiles of CuO, Mn$_2$O$_3$ and Cu-Mn mixed oxide catalysts after calcination in air at 500 °C for 12 h; heating rate 10 °C/min in 5% H$_2$/Ar.**

ment shown in Fig. 1. CuO in both catalysts was reduced at the much lower temperatures, which are 37-47 °C lower than single oxide of CuO. The reduction of Cu-Mn mixed oxide shows similar pattern to that of main component contained in the mixed oxides. However, the reduction occurs at much lower temperature than the corresponding single oxide, indicating that the reducibility of mixed oxide is improved compared to that of single oxide.

The presence of spinel type Cu-Mn oxide phase seems to facilitate the reduction of CuO and $Mn_2O_3$ as indicated by the lower reduction temperature of the components in the Cu-Mn mixed oxide. It may due to the stronger interaction between metal oxide and spinel-type mixed oxide causing interdispersion of the metal oxide. Since small particles are more easily reduced than large ones [28], it may also be due to the particles of different sizes existing in the presence of spinel-type mixed oxide. The high reducibility of Cu-Mn mixed oxide can be ascribed to small metal oxide particles interdispersed with spinel-type mixed oxide.

## 4. Catalytic Activity for Total Oxidation of Propane

The catalytic activity for total oxidation of propane was examined with respect to reaction temperatures as shown in Fig. 5. For all the catalysts, the main reaction product was $CO_2$ and no other carbonaceous products were observed. The activity was in the order of Cu50-Mn50>Cu85-Mn15>$Mn_2O_3$≥Cu15-Mn85>>CuO. Among the Cu-Mn mixed oxides, Cu50-Mn50 with equimolar ratio of Cu to Mn was the most active catalyst, indicating the existence of optimal Cu/Mn ratio. Except Cu15-Mn85 catalyst, the Cu-Mn mixed oxide catalysts show much higher activity than the single oxides such as $Mn_2O_3$ and CuO. Among the catalysts examined, single oxide of CuO revealed the lowest activity. However, the activities of Cu50-Mn50 and Cu85-Mn15 catalysts in which CuO phase was identified as main component are much higher than the single oxide of CuO. It indicates that the existence of spinel type Cu-Mn mixed oxide significantly enhanced the activity of Cu-Mn mixed oxide catalysts. This result also strongly suggests that the coexistence of Cu-Mn mixed oxide and crystalline CuO phases was essential for the high activity for propane oxidation in our catalytic system. Note that the Mn-rich Cu15-Mn85 catalyst without CuO phase revealed

### Table 2. Light-off temperatures ($T_{50}$) corresponding to the conversion of 50% in the total oxidation of propane and BET surface areas

| Catalysts | $T_{50}$ (°C) | $S_{BET}$ ($m^2$/g) |
|---|---|---|
| CuO | 418 | 5.3 |
| $Mn_2O_3$ | 342 | 15.8 |
| Cu15-Mn85 | 356 | 17.0 |
| Cu50-Mn50 | 292 | 46.6 |
| Cu85-Mn15 | 326 | 22.9 |

the lowest activity among the Cu-Mn mixed oxides and lower activity than the single oxide of $Mn_2O_3$. The good activity originates likely from a synergic effect of the CuO and spinel structure of Cu-Mn mixed oxide, because the catalysts containing both phases have high activity for total oxidation of propane. The higher activity of the Cu50-Mn50 catalyst than the Cu85-Mn15 catalyst seems to be due to the smaller crystalline size of CuO in the Cu-Mn mixed oxides as confirmed by XRD. Other researchers [25,29] have discussed similar concepts that the redox of $Cu^{2+}$/$Cu^+$ involves lattice oxygen, while that of $Mn^{3+}$/$Mn^{4+}$ is associated with the adsorption of oxygen species.

The light-off temperatures ($T_{50}$) corresponding to the conversion of 50% and BET surface areas are summarized in Table 2. The BET surface areas of Cu-Mn mixed oxides were in the range of 17.0-46.6 $m^2$/g, which are higher than those of CuO (5.3 $m^2$/g) and $Mn_2O_3$ (15.8 $m^2$/g) single oxides. It may indicate that Cu-Mn mixed oxides prepared by co-precipitation method provide a high dispersion of spinel-type Cu-Mn mixed oxide and the disposition of metal oxides of CuO or $Mn_2O_3$. The activity of the catalysts is well proportional to the BET surface area, indicating that the surface area is partially responsible for the catalytic activity for total oxidation of propane. As confirmed and discussed in $H_2$-TPR measurements, a high dispersion of spinel-type Cu-Mn mixed oxide and the disposition of metal oxides of CuO or $Mn_2O_3$ seems to be related to the easier reducibility of Cu-Mn mixed oxide than the single oxides of CuO or $Mn_2O_3$. The easier reducibility may be one of the reasons for high activity of Cu-Mn mixed oxide for total oxidation of propane.

## CONCLUSIONS

The co-precipitation method for the synthesis of catalysts provides a high interdispersion of copper and manganese metallic elements forming Cu-Mn mixed oxide of spinel structure ($Cu_{1.5}Mn_{1.5}O_4$). Besides the spinel-type Cu-Mn mixed oxide, CuO or $Mn_2O_3$ phases could be formed depending on the Cu/Mn molar ratio of their precursors. Cu-Mn mixed oxides prepared by co-precipitation method show much higher activity for propane oxidation than single CuO and $Mn_2O_3$ oxides. With the increase of Cu/Mn molar ratio, Cu-Mn mixed oxide in spinel phase with the composition of $Cu_{1.5}Mn_{1.5}O_4$ as well as crystalline CuO became dominant oxide phase. The good activity likely originates from a synergic effect of the CuO and spinel structure of Cu-Mn mixed oxide, because the catalysts containing both phases have high activity for total oxidation of propane. Among the mixed oxides, however, Cu50-Mn50 with same metal loading was the most active catalyst, indicating the existence of optimal Cu/Mn ratio. Cu-Mn Mixed oxides were also more reducible than single
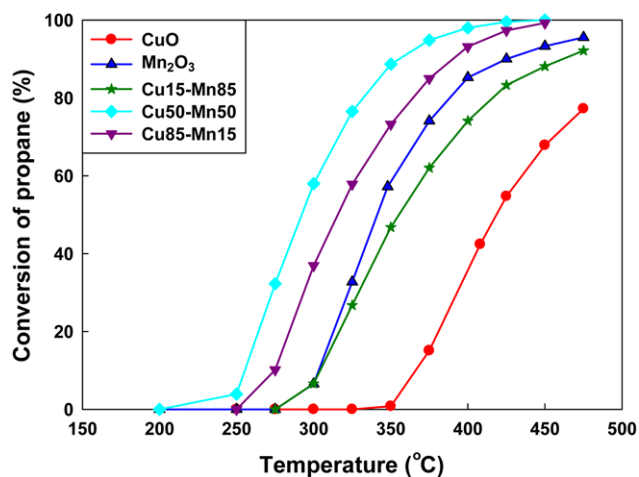


**Fig. 5. Catalytic activity for total oxidation of propane with respect to reaction temperatures; catalyst quantity=0.3 g, gas flow rate=200 $cm^3$/min, $[C_3H_8]$=1%, $[O_2]$=7% in He balance.**

oxides of CuO and $Mn_2O_3$ as observed by $H_2$-TPR. The reducibility seems to be related to the existence of spinel phase of mixed oxides. The easier reducibility and BET surface area seems to be partially responsible for the high activity of Cu-Mn mixed oxides for the total oxidation of propane.

## ACKNOWLEDGEMENT

## REFERENCES

1. A. K. Neyestanaki, N. Kumar and L.-E. Lindfors, *Appl. Catal. B: Environ.*, **7**, 95 (1995).
2. M. Ferrandon, J. Carnö, S. Järås and E. Björnbom, *Appl. Catal. A: Gen.*, **180**, 141 (1999).
3. P. Papaefthimiou, T. Ioannides and X. E. Verykios, *Appl. Catal. B: Environ.*, **15**, 75 (1998).
4. M. R. Morales, B. P. Barbero and L. E. Cadùs, *Appl. Catal. B: Environ.*, **67**, 229 (2006).
5. P. Marècot, A. Fakche, B. Kellali, G. Mabilon, M. Prigent and J. Barbier, *Appl. Catal. B: Environ.*, **3**, 283 (1994).
6. T. F. Garetto, E. Rincón and C. R. Apesteguia, *Appl. Catal. B: Environ.*, **48**, 167 (2004).
7. Y. Yazawa, N. Takagi, H. Yoshida, S. Komai and A. Satsuma, T. Tanaka, S. Yoshida and T. Hattori, *Appl. Catal. A: Gen.*, **233**, 103 (2002).
8. J. Carnö, M. Ferrandon, E. Björnbom and S. Järås, *Appl. Catal. A: Gen.*, **155**, 265 (1997).
9. R. Craciun, B. Nentwick, K. Hadjiivanov and H. Knözinger, *Appl. Catal. A: Gen.*, **243**, 67 (2003).
10. A. A. Mirzaei, H. R. Shaterian and M. Kaykhaii, *Appl. Sur. Sci.*, **239**, 246 (2005).
11. G. Fortunato, H. R. Oswald and A. Reller, *J. Mater. Chem.*, **11**, 905 (2001).
12. M. Krämer, T. Schmidt, L. Stöwe and W. F. Maier, *Appl. Catal. A: Gen.*, **302**, 257 (2006).
13. C. Jones, K. J. Coles, S. H. Taylor, M. J. Crudace and G. J. Hutchings, *J. Mol. Catal. A.*, **305**, 121 (2009).
14. E. C. Njagi, C. H. Chen, H. Genuino, H. Galindo, H. Huang and S. L. Suib, *Appl. Catal. B: Environ.*, **99**, 103 (2004).
15. G. J. Hutchings, A. A. Mirzaei, M. R. H. Siddiqui and S. H. Taylor, *Appl. Catal. A: Gen.*, **166**, 143 (1998).
16. S. B. Kanungo, *J. Catal.*, **58**, 419 (1979).
17. H. Chen, X. Tong and Y. Li, *Appl. Catal. A: Gen.*, **370**, 59 (2009).
18. A. Wöllner, F. Lange, H. Schmelz and H. Knözinger, *Appl. Catal. A: Gen.*, **94**, 181 (1993).
19. I. Spassova, M. Khristova, D. Panayotov and D. Mehandjiev, *J. Catal.*, **185**, 43 (1999).
20. K. Zhi, Q. Liu, Y. Zhang, S. He and R. He, *J. Fuel Chem. Technol.*, **38**(4), 445 (2010).
21. Y. Tanaka, T. Takeguchi, R. Kikuchi and K. Eguchi, *Appl. Catal. A: Gen.*, **279**, 59 (2005).
22. A. P. B. Sinha, N. R. Sanjana and A. B. Biswas, *J. Phys. Chem.*, **62**, 191 (1958).
23. S. Miahara, *J. Phys. Soc. Jpn.*, **17B-I**, 181 (1962).
24. G. B. Lasse, *J. Phys. Chem. Solids*, **27**, 383 (1966).
25. S. Veprek, D. L. Cocke, S. Kehl and H. R. Oswald, *J. Catal.*, **100**, 250 (1986).
26. B. Solsona and T. E. Davies, *Appl. Catal. B: Environ.*, **84**, 176 (2008).
27. I. R. Leith and M. G. Howden, *Appl. Catal.*, **37**, 75 (1992).
28. S. J. Gentry, N. W. Hurst and A. Jones, *J. Chem. Soc. Faraday Trans. I*, **77**, 603 (1981).
29. F. C. Buciuman and F. Patcas, *Chem. Eng. Process.*, **38**, 569 (1999).